Science in China Series A: Mathematics
Aug., 2008, Vol. 51, No. 8, 1522–1536
www.scichina.com math.scichina.com
www.springerlink.com

Calculating the vertex unknowns of nine point scheme on quadrilateral meshes for diffusion equation

YUAN GuangWei† & SHENG ZhiQiang

Laboratory of Computational Physics, Institute of Applied Physics and Computational Mathematics, P. O. Box 8009, Beijing 100088, China
(email: yuan_guangwei@iapcm.ac.cn)

Abstract In the construction of nine point scheme, both vertex unknowns and cell-centered unknowns are introduced, and the vertex unknowns are usually eliminated by using the interpolation of neighboring cell-centered unknowns, which often leads to lose accuracy. Instead of using interpolation, here we propose a different method of calculating the vertex unknowns of nine point scheme, which are solved independently on a new generated mesh. This new mesh is a Voronoï mesh based on the vertexes of primary mesh and some additional points on the interface. The advantage of this method is that it is particularly suitable for solving diffusion problems with discontinuous coefficients on highly distorted meshes, and it leads to a symmetric positive definite matrix. We prove that the method has first-order convergence on distorted meshes. Numerical experiments show that the method obtains nearly second-order accuracy on distorted meshes.

Keywords: diffusion equation, nine point scheme, distorted meshes, Voronoï meshes

MSC(2000): 65M06, 65M12, 65M55

1 Introduction

Accurate and efficient discretization methods for the diffusion equation on distorted meshes are very important for the numerical simulations of Lagrangian hydrodynamics and magnetohydrodynamics. The finite volume method is widely used in practical problems such as computational fluid dynamics. Moreover, it is flexible enough to be applied to complex space domains, and because it works directly on the physical domain rather than on the computational domain through coordinate transformations, it can be easily used in solving radiation hydrodynamic equations that describe certain physical motion or change with large amplitude.

The finite volume scheme on admissible meshes were presented and discussed in [1, 2]. But, the admissible meshes are a kind of very special meshes, and in some problems such as Lagrangian radiation hydrodynamics the computational meshes become distorted meshes, which are not admissible meshes.

Received March 14, 2008; accepted May 9, 2008
DOI: 10.1007/s11425-008-0108-x
† Corresponding author
This work was partially supported by the National Basic Research Program (Grant No. 2005CB321703), the National Nature Science Foundation of China (Grant No. 90718029), and the Basic Research Project of National Defense (Grant No. A1520070074)

A finite volume scheme for solving diffusion equations on non-rectangular meshes was proposed in [3], which is the so-called nine point scheme on arbitrary quadrilateral meshes. Both vertex unknowns and cell-centered unknowns were at first introduced in the construction of the nine point scheme, and then the vertex unknowns were usually eliminated by taking them as the arithmetic average of the neighboring cell-centered unknowns due to the consideration of computational cost. Thus this scheme has only cell-centered unknowns after the interpolation. Unfortunately, this simple interpolation loses significant accuracy on moderately and highly skewed meshes, especially for transient problems with large gradients. Some similar finite volume schemes were discussed in [4–6].

The support operators method (SOM) in [7, 8] gave second-order accuracy on both smooth and nonsmooth meshes either with or without material discontinuities, and they generally lead to a symmetric positive definite matrix. However, there is no explicit expression for the discrete normal flux on cell edge, and both cell-edged unknowns and cell-centered unknowns are used.

The method of multipoint flux approximations[9] (MPFA) has only cell-centered unknowns and gives an explicit expression for the face-centered flux. However, it generally leads to a nonsymmetric matrix, and does not satisfy the discrete maximum principle.

The scheme in [10] has both cell-centered unknowns and vertex unknowns, and leads to a symmetric positive definite matrix. Although numerical experiments show that this scheme indeed has second-order accuracy, no theoretical proof is given. In [11], the authors analyzed the scheme theoretically, and gave a construction of a finite volume scheme for diffusion equations with discontinuous coefficients.

In [12], the authors presented a method of eliminating vertex unknowns in the nine point scheme for discretizing diffusion operators on distorted quadrilateral meshes, in which the vertex unknowns are expressed as the interpolation of neighboring cell-centered unknowns based on certain rigorous derivation. The resulting scheme has only the cell-centered unknowns and has a local stencil. However, it leads to a nonsymmetric matrix in general.

In this paper, we will present a new method of computing the vertex unknowns in nine point scheme. First, we generate a Voronoï mesh (or dual Delaunay mesh) based on the vertexes of primary mesh and some additional points, where the motivation of adding points will be explained, and a criteria of adding points and an algorithm of additive process are proposed. Then we construct a finite volume scheme on the Voronoï mesh, whose cell-centers, except for the points added, are the vertex of the primary mesh. Finally we solve the cell-centered unknowns of primary meshes using the nine point scheme on the primary mesh. Our scheme leads to a symmetric positive definite matrix, and we will prove that it gives first-order convergence.

The rest of this paper is organized as follows: In Section 2, we describe the Voronoï mesh generation and the construction of our scheme for diffusion problems. In Section 3, we prove that the scheme has first-order accuracy. Then we present some numerical experiments to show their performance on several test problems in Section 4. Finally the conclusion is given in Section 5.

2 Construction of scheme for diffusion equation

2.1 Problem and assumption

Consider the following diffusion problem

$$u_t - \nabla \cdot (\lambda(x,t)\nabla u) = f(x,t), \quad \text{in} \quad \Omega \times (0,T], \tag{2.1}$$

$$u(x,t) = 0, \quad \text{on} \quad \partial\Omega \times [0,T], \tag{2.2}$$

$$u(x,0) = \varphi(x), \quad \text{on} \quad \Omega, \tag{2.3}$$

where Ω is an open bounded polygonal set of R^2 with boundary $\partial\Omega$, $\lambda(x,t)$ is the diffusion coefficient, $f = f(x,t)$ is the source term, and φ is the initial value function.

Denote $\Omega = \Omega_1 \cup \Gamma \cup \Omega_2$, where Ω_1 and Ω_2 are two disjoint polygons, Γ is a discontinuous line inside Ω. We need the following assumptions:

(I) $\lambda(x,t) \in C(\overline{\Omega}_i \times [0,T])$ $(i = 1,2)$, $\lambda(x,t)$ is discontinuous at $\Gamma \times [0,T]$.

(II) $f(x,t) \in C(\overline{\Omega}_i \times [0,T])$ $(i = 1,2)$, $\varphi(x) \in C(\overline{\Omega})$, and $\varphi(x) = 0$ for $x \in \partial\Omega$.

(III) The problem (2.1)–(2.3) has a unique solution $u(x,t) \in C^{2,1}(\overline{\Omega}_i \times [0,T])$ $(i = 1,2)$, and $u(x,t) \in C(\overline{\Omega} \times [0,T])$ and the normal flux $\lambda(x,t)\nabla u(x,t) \cdot \vec{n}$ is continuous across $\overline{\Gamma} \times [0,T]$.

For the sake of clarity, we describe briefly the construction of the nine point scheme (also see [3, 12]).

2.2 Nine point scheme

We will use the similar notations as [12]. The domain Ω is divided by a mesh (called primary mesh) made up of arbitrary quadrilateral cells, and Γ consisting of some edges of primary mesh cells. For the primary mesh, we denote the (primary) cells and cell-centers by K and L, the vertexes by p and q, and the cell side by σ (see Figure 1). If the cell side σ is a common edge of cells K and L, and its vertices are p and q, then we denote $\sigma = K|L = pq$.

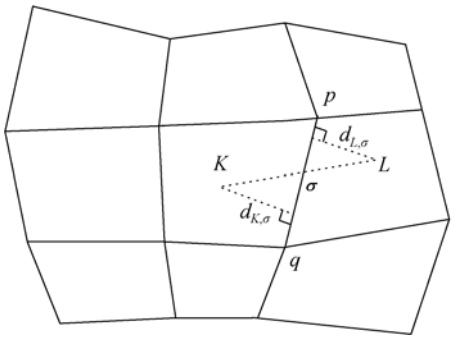

Figure 1 Stencil

Let $\mathcal{J}$ be the set of all (primary) cells, $\mathcal{E}$ be the set of all cell edges, $\mathcal{E}_{\text{int}}$ be the set of all cell edges not on $\partial\Omega$, $\mathcal{E}_{\text{ext}}$ be the set of all cell edges on $\partial\Omega$, and $\mathcal{E}_K$ be the set of all cell edges of cell K. Denote $\mathcal{E}_{\text{int}}^o = \{\sigma \in \mathcal{E}_{\text{int}} : \sigma \cap \partial\Omega = \emptyset\}$, and $h = (\sup_{K\in\mathcal{J}} m(K))^{1/2}$, where $m(K)$ is the area of cell K.

Discretize the time segment by $0 = t^0 < t^1 < \cdots < t^{N+1} = T$, and denote $t^n = n\Delta t$ $(n = 0, 1, \ldots, N+1)$.

With these notations, the nine point scheme can be written as follows[3, 12]:

$$m(K)\frac{u_K^{n+1} - u_K^n}{\Delta t} + \sum_{\sigma\in\mathcal{E}_K} F_{K,\sigma}^{n+1} = m(K) f_K^{n+1}, \quad \forall\, K \in \mathcal{J}, \quad 0 \leqslant n \leqslant N, \tag{2.4}$$

where the discrete normal edge-flux on $\sigma = K|L = qp$ is

$$F_{K,\sigma}^{n+1} = \begin{cases} -\tau_\sigma^{n+1}[u_L^{n+1} - u_K^{n+1} - D_\sigma(u_p^{n+1} - u_q^{n+1})], & \text{if } \sigma \in \mathcal{E}_{\text{int}}^o, \\ -\tau_\sigma^{n+1}(u_L^{n+1} - u_K^{n+1} - D_\sigma u_p^{n+1}), & \text{if } \sigma \in \mathcal{E}_{\text{int}} \text{ and } q \in \partial\Omega, \\ -\tau_\sigma^{n+1}(u_L^{n+1} - u_K^{n+1} + D_\sigma u_q^{n+1}), & \text{if } \sigma \in \mathcal{E}_{\text{int}} \text{ and } p \in \partial\Omega, \\ \tau_\sigma^{n+1} u_K^{n+1}, & \text{if } \sigma \in \mathcal{E}_{\text{ext}}, \end{cases}$$

and

$$f_K^{n+1} = \frac{1}{m(K)} \int_K f(x, t^{n+1}) dx.$$

The notations in the expression of discrete normal edge-flux are defined in the following:

$$\tau_\sigma^{n+1} = \frac{m(\sigma)}{\frac{d_{L,\sigma}}{\lambda_{L,\sigma}^{n+1}} + \frac{d_{K,\sigma}}{\lambda_{K,\sigma}^{n+1}}}, \qquad D_\sigma = \frac{(L-K, p-q)}{|\sigma|^2},$$

where $d_{L,\sigma} = \text{dist}\,(L, \sigma)$, $d_{K,\sigma} = \text{dist}\,(K, \sigma)$, $\lambda_{L,\sigma}^{n+1} = \frac{1}{m(\sigma)} \int_\sigma \lambda^+(x, t^{n+1}) dl$, $\lambda_{K,\sigma}^{n+1} = \frac{1}{m(\sigma)} \int_\sigma \lambda^-(x, t^{n+1}) dl$, $\lambda^+(x, t^{n+1}) = \lambda(x, t^{n+1})|_K$, and $\lambda^-(x, t^{n+1}) = \lambda(x, t^{n+1})|_L$.

The discrete initial condition is taken as follows:

$$u_K^0 = \varphi_K \equiv \frac{1}{m(K)} \int_K \varphi(x) dx, \quad \forall\, K \in \mathcal{J}. \tag{2.5}$$

It is obvious that there are vertex unknowns u_p^{n+1} and u_q^{n+1} in addition to cell-centered unknowns u_K^{n+1} and u_L^{n+1} in the expressions of the normal flux component. Usually the vertex unknowns will be eliminated by locally approximating them with surrounding cell-centered unknowns. On quadrilateral meshes it results in a finite volume scheme with nine point stencil so that it is named as nine point scheme. A lot of numerical results show that the computation of vertex unknowns remarkably affects the accuracy of nine point scheme. Hence, it is a key question how to eliminate the vertex unknowns. Some methods of eliminating the vertex unknowns by using the cell-centered unknowns were presented in [6, 12]. In this paper, we will compute directly the vertex unknowns of primary meshes by using the Voronoï tessellation, which will be described in details in the next subsection.

2.3 Method of computing the vertex unknowns

In this subsection and the following we define the interface I as the union of the boundary of domain $\partial\Omega$ and the discontinuous line Γ. For the definition and conclusion about Voronoï mesh and Delaunay triangle we refer to [13].

First, we generate a Voronoï mesh, whose cell-centers are the vertexes of primary mesh and some additional points on I. These cell-centers will be called as site points, and they are the vertexes of the dual Delaunay mesh (see [13]). We add some points at the interface in order to ensure that the interface keeps standing on the edges of the Delaunay mesh. It follows that the edges of each Voronoï cell with centers being at the interface, are orthogonal to the interface. Then a cell-centered finite volume scheme can be easily constructed on this Voronoï mesh[1, 2]. It is worth pointing out that the cell-centered unknowns of primary mesh do not be used in this scheme on the Voronoï mesh generated.

Now we explain furthermore the construction of our Voronoï mesh. If we generate a Voronoï mesh with only the vertexes of primary meshes, and without adding points on I, then we obtain a dual Delaunay mesh whose edges maybe not include all edges on the interface. That is, some edges on the interface could be deleted and don't appear in the Delaunay mesh generated. It leads to mixed cells (with discontinuity inside the interior of cell) with complex shape so that it is difficult to construct a scheme on these mixed cells. Therefore, in order to avoid mixed cells with complex shape for solving diffusion equations with discontinuous coefficients, we must ensure that the interface do not be damaged. In other words we will generate a Voronoï mesh

(and the dual Delaunay mesh), based on site points including the vertexes of primary mesh and some additional points on I, to ensure all edges on the interface are some edges in the Delaunay mesh.

Next, we give an algorithm of adding points in the interface to generate the Voronoï mesh required. Let $h_0 = \frac{1}{2}\min\{l_1, l_2\}$, where l_1 is the minimum of the distances from the vertex points outside the interface to the interface, and l_2 is the minimum of length of primary cell edge on the interface.

Let ϑ be the angle of neighboring two cell-edges of primary cell (one of which lies on the interface), and ϑ_0 be the minimum of ϑ.

When $\frac{\pi}{2} \leqslant \vartheta \leqslant \pi$, the Voronoï cell associated with a site point added in one edge of the interface does not across another edge of primary cell. It remains to consider the case $0 < \vartheta < \frac{\pi}{2}$.

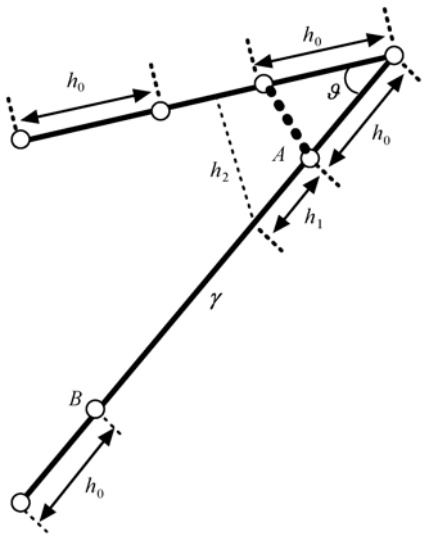

Figure 2 The method adding points on interface

We first add two points for each edge in interface, so that the distances from the added point to the near vertex of the edge are h_0 (see Figure 2). For example, two added points are A and B for the primary cell edge γ ($\gamma \subset I$). Denote the length of the edge γ be H, and thus the length of AB is $H - 2h_0$. Two cases are distinguished according to the length H.

(i) If $2h_0 < H < 3h_0$, then it is unnecessary to add any more points.

(ii) If $H \geqslant 3h_0$, then $\frac{H}{h_0} - 2 \geqslant 1$. Hence, there is a positive integer m, such that

$$\frac{1-\sin\vartheta_0}{\sin\vartheta_0}\left(\frac{H}{h_0}-2\right) \leqslant m \leqslant \frac{1}{\sin\vartheta_0}\left(\frac{H}{h_0}-2\right).$$

Denote $c_0 = \frac{1}{m}(\frac{H}{h_0} - 2)$ and $h_1 = c_0 h_0$. There are $\sin\vartheta_0 \leqslant c_0 \leqslant \frac{\sin\vartheta_0}{1-\sin\vartheta_0}$, $mh_1 = H - 2h_0$, and $h_1 \leqslant \frac{h_0\sin\vartheta_0}{1-\sin\vartheta_0}$. Hence, there is $(h_1+h_0)\sin\vartheta \geqslant h_1$. We add uniformly $m-1$ points in the segment AB with step-length h_1, in other words, the segment AB is divided into m sub-segments and the length of each sub-segment is h_1. Hence, we add $m+1$ points in the segment γ. For different cell edges, m may be different. It is obvious that all of the circles with diameter being these sub-segments do not include any other site points.

Now we define the site point set $P = \{p_i\}$ which consists of the vertexes of primary mesh and the points added on I according to the above algorithm of additive process. For any point q, denote $C_P(q)$ be the maximum circle which includes no other site points of P, and the center of circle is q.

Let $\mathrm{Vor}(P)$ be the Voronoï tessellation associated with the set P, and $\mathcal{V}(P)$ be the corresponding Voronoï mesh with Voronoï cells being restricted within $\overline{\Omega}$. And $\mathcal{DG}(P)$ is the dual Delaunay triangle mesh associated with P.

We need the following lemma (see [13]):

Lemma 1. (i) *For* $\mathrm{Vor}(P)$ *associated with the set* P*, the sufficient and necessary condition that the perpendicular bisector of segment* p_ip_j *determining one edge of* $\mathrm{Vor}(P)$ *are that there is a point* q *in this segment, such that the boundary of* $C_P(q)$ *includes points* p_i *and* p_j*, and includes no other site points.*

(ii) *The sufficient and necessary condition that the segment* p_ip_j *is one edge of* $\mathcal{DG}(P)$ *are that there exists a closed disk* C_{ij}*, whose boundary includes* p_i *and* p_j*, and no other site points of* P*.*

By using our method of adding points in the interface I and Lemma 1, we get the following result.

Lemma 2. *If we add appropriately some site points in the interface, then all the segments on the interface are the edges of the Delaunay triangle mesh whose vertexes are the vertexes of primary mesh and these points added on the interface* I*.*

Now we introduce some notations. Denote the cell and cell center of Voronoï mesh by $p, q, \ldots$, the vertex of Voronoï mesh by A and B, and the cell side of Voronoï cell by γ (see Figure 3). If the cell side γ is a common edge of (Voronoï) cells p and q, and its vertices are A and B, then we denote $\gamma = p|q = BA$. And let $P_{\mathrm{int}} = P \cap \Omega$, and $\mathcal{VE}_{\mathrm{int}} = \{\gamma | \gamma \in \partial p, p \in P_{\mathrm{int}}\}$.

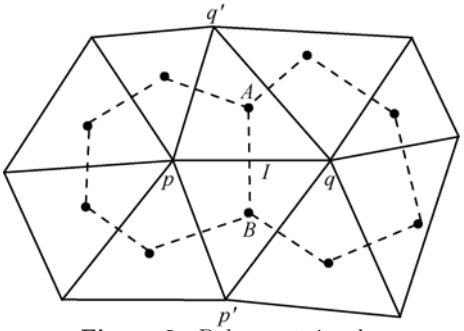

Figure 3 Delaunay triangle

Note that the set P and Voronoï mesh satisfy the definition of admissible meshes presented in [1], and the finite volume scheme on admissible meshes have been discussed in [1, 2]. Then the finite volume scheme on the Voronoï mesh is as follows:

$$m(p)\frac{u_p^{n+1} - u_p^n}{\Delta t} + \sum_{\gamma \in \partial p} F_{p,\gamma}^{n+1} = m(p) f_p^{n+1}, \quad p \in P_{\mathrm{int}}, \tag{2.6}$$

$$u_p^{n+1} = 0, \quad p \in \partial\Omega, \tag{2.7}$$

$$u_p^0 = \varphi(p), \quad p \in P. \tag{2.8}$$

Here $F_{p,\gamma}^{n+1} = -\xi_\gamma^{n+1}(u_q^{n+1} - u_p^{n+1})$, where

$$\xi_\gamma^{n+1} = \frac{1}{|qp|}\int_\gamma \lambda(x, t^{n+1}) dl.$$

By solving the system (2.6)–(2.8), we can get the values u_p^{n+1} defined on site points, which include the vertex of primary mesh. With the values of vertex unknowns of primary mesh being known, and substituting them into the nine point scheme (2.4), we obtain a system with only cell-centered unknowns $\{u_K^{n+1}\}$ on the primary mesh.

Remark. If we use the cell-centers of the primary mesh and the points added on the interface I as site points to generate a Voronoï mesh, and on this mesh apply the similar finite volume scheme with (2.6)–(2.8) to get the cell-centered values of this Voronoï mesh, then it seems that

the unknowns located at the cell-centers of the primary mesh can be obtained directly, and half of the computational cost should be reduced. However the cell-centered values of this Voronoï mesh are different from the cell-centered unknowns $\{u_K^{n+1}\}$ solved by (2.6)–(2.8) on the primary mesh, both in physical meaning and in mathematical conception. It is worth to point out the scheme, that we hope to construct, should be suitable to compute Lagrangian hydrodynamic problems coupled with radiation diffusion, and the primary mesh comes from Lagrangian cells in hydrodynamics. So the cell-centered unknowns $\{u_K^{n+1}\}$ have to be defined as well as solved on the primary mesh, which represent the average temperatures on the Lagrangian cells other than on different cells of any other mesh.

Note that in this paper the vertex unknowns of nine point scheme are defined on the vertexes of the primary mesh. They can be regarded as the temperature values defined on the vertexes and calculated on a new generated mesh. Usually they are auxiliary (though very important sometimes) in solving the cell-centered scheme (2.4) on the primary mesh.

3 Convergence of scheme

In this section, we will prove that our scheme is convergent. First, we prove that the scheme on Voronoï mesh is convergent.

3.1 Convergence result on Voronoï mesh

The finite volume scheme on Voronoï mesh has been discussed in [1, 2], but here we give the convergent result for completeness.

By integrating (2.1) over the Voronoï cell p and using the Green formula, one obtains

$$\int_p u_t(x,t^{n+1})dx + \sum_{\gamma\in\partial p} \mathbf{F}_{p,\gamma}^{n+1} = \int_p f(x,t^{n+1})dx, \tag{3.1}$$

where $\mathbf{F}_{p,\gamma}^{n+1}$ is the normal flux on the edge γ of Voronoï cell p, defined by

$$\mathbf{F}_{p,\gamma}^{n+1} = -\int_\gamma \lambda(x,t^{n+1})\nabla u(x,t^{n+1})\cdot\vec{n}_{p,\gamma}dl. \tag{3.2}$$

Here ∂p is the boundary of Voronoï cell p, and $\vec{n}_{p,\gamma}$ is the outward unit normal on the edge γ. For simplicity, we will omit the variables t and t^{n+1} if no confusion occurs.

By the Taylor expansion, one has

$$u(q)-u(p) = \nabla u(x)\cdot(q-p) + \int_0^1 (H_q - H_p)sds,$$

where $H_q = (\nabla^2 u(sx+(1-s)q)(q-x), q-x)$, $\nabla^2 u(sx+(1-s)q)$ is the Hessian matrix of u at the point $sx+(1-s)q$, the notation H_p has similar meaning. It follows that

$$\frac{u(q)-u(p)}{|qp|}\int_\gamma \lambda(x)dl = \int_\gamma \lambda(x)\nabla u(x)\cdot\vec{n}_{p,\gamma}dl + \int_\gamma \frac{\lambda(x)}{|qp|}\int_0^1 (H_q-H_p)sdsdl,$$

By the assumption (III), there is

$$\int_\gamma \frac{\lambda(x)}{|qp|}\int_0^1 (H_q-H_p)sdsdl = O(h^2),$$

where $h = \max(\mathrm{diam}\mathcal{V}(P), \mathrm{diam}\mathcal{J})$, $\mathrm{diam}\mathcal{V}(P)$ and $\mathrm{diam}\mathcal{J}$ are the maximum of the diameters of cells in $\mathcal{V}(P)$ and $\mathcal{J}$ respectively.

Introduce the following assumption:

Assumption (IV) For any edge $\gamma = BA = p|q$ of Voronoï cell, there is a constant $C > 0$, such that $|BA| \leqslant C|qp|$.

Equation (3.1) can be rewritten to

$$m(p)\frac{u(p,t^{n+1}) - u(p,t^n)}{\Delta t} + \sum_{\gamma\in\partial p} \overline{F}_{p,\gamma}^{n+1} = m(p)f_p^{n+1} - S_p^{n+1} + \sum_{\gamma\in\partial p} m(\gamma)R_{p,\gamma}^{n+1}, \quad p \in P_{\mathrm{int}}, \tag{3.3}$$

where $m(p)f_p^{n+1} = \int_p f(x,t^{n+1})dx$, $\overline{F}_{p,\gamma}^{n+1} = -\xi_\gamma^{n+1}(u(q,t^{n+1}) - u(p,t^{n+1}))$, $m(\gamma)R_{p,\gamma}^{n+1} = \overline{F}_{p,\gamma}^{n+1} - \mathbf{F}_{p,\gamma}^{n+1}$, $S_p^{n+1} = \int_p s_p^{n+1}(x)dx$, $s_p^{n+1}(x) = u_t(x,t^{n+1}) - \frac{u(p,t^{n+1})-u(p,t^n)}{\Delta t}$, $|s_p^{n+1}(x)| \leqslant C(\Delta t + h)$, and $|S_p^{n+1}| \leqslant Cm(p)(\Delta t + h)$. It follows that, when $|BA|/|qp| = O(1)$, there holds

$$|\overline{F}_{p,\gamma}^{n+1} - \mathbf{F}_{p,\gamma}^{n+1}| = O(h^2).$$

Let $e_p^n = u(p,t^n) - u_p^n$, and $G_{p,\gamma}^{n+1} = \overline{F}_{p,\gamma}^{n+1} - F_{p,\gamma}^{n+1} = -\xi_\gamma^{n+1}(e_q^{n+1} - e_p^{n+1})$. Then there are

$$m(p)\frac{e_p^{n+1} - e_p^n}{\Delta t} + \sum_{\gamma\in\partial p} \overline{G}_{p,\gamma}^{n+1} = -S_p^{n+1} + \sum_{\gamma\in\partial p} m(\gamma)R_{p,\gamma}^{n+1}, \quad p \in P_{\mathrm{int}}, \tag{3.4}$$

$$e_p^{n+1} = 0, \quad p \in \partial\Omega, \tag{3.5}$$

$$e_p^0 = \varphi(p) - \varphi_p, \quad p \in P. \tag{3.6}$$

Multiplying (3.4) by e_p^{n+1}, and summing up the resulting products for $p \in P_{\mathrm{int}}$, we get

$$\begin{aligned}\frac{1}{\Delta t}\sum_{p\in P_{\mathrm{int}}} m(p)(e_p^{n+1} - e_p^n)e_p^{n+1} + \sum_{p\in P_{\mathrm{int}}}\sum_{\gamma\in\partial p} \overline{G}_{p,\gamma}^{n+1}e_p^{n+1} \\ = -\sum_{p\in P_{\mathrm{int}}} S_p^{n+1}e_p^{n+1} + \sum_{p\in P_{\mathrm{int}}}\sum_{\gamma\in\partial p} m(\gamma)R_{p,\gamma}^{n+1}e_p^{n+1}.\end{aligned} \tag{3.7}$$

Notice that $R_{p,\gamma}^{n+1} = -R_{q,\gamma}^{n+1}$ for $\gamma = p|q$; $\nabla_\gamma e^{n+1} = 0$ for $\gamma \subset \partial\Omega$; $e_p^{n+1} = 0$ for $p \in \partial\Omega$. The above equation can be rewritten to

$$\begin{aligned}\frac{1}{2\Delta t}\sum_{p\in P_{\mathrm{int}}} m(p)(|e_p^{n+1}|^2 - |e_p^n|^2) + \sum_{\gamma\in\mathcal{VE}_{\mathrm{int}}} \xi_\gamma^{n+1}(e_q^{n+1} - e_p^{n+1})^2 \\ \leqslant \sum_{p\in P_{\mathrm{int}}} |S_p^{n+1}||e_p^{n+1}| + \sum_{\gamma\in\mathcal{VE}_{\mathrm{int}}} m(\gamma)R_\gamma^{n+1}\nabla_\gamma e^{n+1},\end{aligned} \tag{3.8}$$

where $\nabla_\gamma e_p^{n+1} = |e_q^{n+1} - e_p^{n+1}|$ and $R_\gamma^{n+1} = |R_{p,\gamma}^{n+1}|$. It is obvious that there is a constant C depending on u and $\frac{1}{|\gamma|}\int_\gamma \lambda(x,t^{n+1})dl$, such that

$$\sum_{\gamma\in\mathcal{E}_{\mathrm{int}}} \frac{(|\gamma|R_\gamma^{n+1})^2}{\xi_\gamma^{n+1}} \leqslant Ch^2. \tag{3.9}$$

Define the discrete L^2-norm and H^1-seminorm as follows:

$$\|e^n\|_2^2 = \sum_{p\in P} m(p)|e_p^n|^2, \qquad \|\nabla_\gamma e^n\|_2^2 = \sum_{\gamma\in\mathcal{VE}_{\mathrm{int}}} \xi_\gamma^{n+1}|\nabla e^n|^2.$$

By (3.8), (3.9) and the Cauchy inequality, one has

$$\frac{1}{2\Delta t}\left(\|e^{n+1}\|_2^2-\|e^n\|_2^2\right)+\|\nabla_\gamma e^{n+1}\|_2^2\leqslant\frac{1}{2}\|e^{n+1}\|_2^2+\frac{1}{2}\|\nabla_\gamma e^{n+1}\|_2^2+C(h+\Delta t)^2.$$

Hence,

$$\|e^{n+1}\|_2^2+\frac{1}{1-\Delta t}\|\nabla_\gamma e^{n+1}\|_2^2\Delta t\leqslant\frac{1}{1-\Delta t}\|e^n\|_2^2+\frac{C\Delta t}{1-\Delta t}(h+\Delta t)^2.$$

When $\Delta t\leqslant\frac{1}{2}$, we apply the discrete Gronwall inequality to obtain

$$\|e^{n+1}\|_2^2+\sum_{k=0}^{n}\|\nabla_\gamma e^{k+1}\|_2^2\Delta t\leqslant C(h+\Delta t)^2,\quad 0\leqslant n\leqslant N. \tag{3.10}$$

Thus, we obtain the following convergent result:

Lemma 3. *For the scheme* (2.6)–(2.8), *there exists a constant* C, *independent of* h, *such that*

$$\|e^{n+1}\|_2^2+\sum_{k=0}^{n}\|\nabla_\gamma e^{k+1}\|_2^2\Delta t\leqslant C(h+\Delta t)^2,\quad 0\leqslant n\leqslant N.$$

3.2 Convergence result on primary mesh

Now we present an error estimate for the scheme on primary mesh $\mathcal{J}$. By our method of adding points, we can know that $m+1$ points $\{p_i\in\sigma|i=1,2,\ldots,m+1\}$ are added in the interface $\sigma=qp$ (see Figure 4). For $1\leqslant i\leqslant m+2$, denote $\sigma_i=p_{i-1}p_i$, and $\tau_{\sigma_i}^{n+1}=\frac{1}{|\sigma_i|}\int_{B_iA_i}\lambda(x,t^{n+1})dl$, B_iA_i is the common edge of the Voronoï cells p_{i-1} and p_i. For a (interior) cell edge $\sigma=qp$ of primary meshes satisfying $|\sigma\cap I|=0$, there are m' edges $\sigma_i=q_iq_{i-1}$ $(1\leqslant i\leqslant m')$ of Delaunay mesh such that $q_0=p,q_{m'}=q$. And let $\gamma_i=q_i|q_{i-1}$ $(1\leqslant i\leqslant m')$.

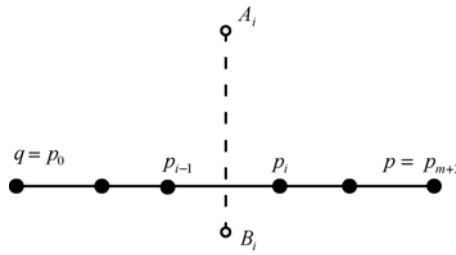

Figure 4 The points added in interface

Introduce the following assumption:

Assumption (V) There are positive constants C and M, such that $m'\leqslant M$, and

$$\tau_\sigma^{n+1}|D_\sigma|^2\quad\leqslant\quad C\xi_{\gamma_i}^{n+1},\ \text{ for } 1\leqslant i\leqslant m',\sigma\in\mathcal{E}\setminus I,\ \text{ and for } 1\leqslant i\leqslant m+1,\sigma\in I.$$

By integrating (2.1) over the primary cell K and using the Green formula, one obtains

$$\int_K u_t(x,t^{n+1})dx+\sum_{\sigma\in\partial K}\mathbf{F}_{K,\sigma}^{n+1}=\int_K f(x,t^{n+1})dx, \tag{3.11}$$

where

$$\mathbf{F}_{K,\sigma}^{n+1}=-\int_\sigma\lambda(x,t^{n+1})\nabla u(x,t^{n+1})\cdot\vec{n}_{K,\sigma}dl.$$

Define the flux $\overline{F}_{K,\sigma}^{n+1}$ as follows:

$$\overline{F}_{K,\sigma}^{n+1} = \begin{cases} -\tau_\sigma \left[u(L) - u(K) - D_\sigma(u(p) - u(q))\right], & \text{if } \sigma = K|L = qp \in \mathcal{E}_{\text{int}}^o, \\ -\tau_\sigma \left[u(L) - u(K) - D_\sigma u(p)\right], & \text{if } \sigma = K|L = qp \in \mathcal{E}_{\text{int}}, \text{and } q \in \partial\Omega, \\ -\tau_\sigma \left[u(L) - u(K) + D_\sigma u(q)\right], & \text{if } \sigma = K|L = qp \in \mathcal{E}_{\text{int}}, \text{and } p \in \partial\Omega, \\ \tau_\sigma u(K), & \text{if } \sigma = K|L = qp \in \mathcal{E}_{\text{ext}}. \end{cases}$$

Here the variables t and the superscript $n+1$ are ignored. And let

$$S_K^{n+1} = \int_K s_K^{n+1}(x)dx,$$

where

$$s_K^{n+1}(x) = u_t(x, t^{n+1}) - \frac{u(K, t^{n+1}) - u(K, t^n)}{\Delta t}.$$

It is easy to see that $|S_K^{n+1}| \leqslant C(h + \Delta t)m(K)$.

The equation (3.11) can be rewritten to

$$m(K)\frac{u(K, t^{n+1}) - u(K, t^n)}{\Delta t} + \sum_{\sigma\in\mathcal{E}_K} \overline{F}_{K,\sigma}^{n+1} = m(K)f_K^{n+1} - S_K^{n+1} + \sum_{\sigma\in\mathcal{E}_K} m(\sigma)R_{K,\sigma}^{n+1}, \quad (3.12)$$

where $m(\sigma)R_{K,\sigma}^{n+1} = \overline{F}_{K,\sigma}^{n+1} - \mathbf{F}_{K,\sigma}^{n+1}$.

Let $E_K^n = u(K, t^n) - u_K^n$, $e_p^n = u(p, t^n) - u_p^n$, and $G_{K,\sigma}^{n+1} = \overline{F}_{K,\sigma}^{n+1} - F_{K,\sigma}^{n+1}$. By (2.4) and (3.12), there holds

$$m(K)\frac{E_K^{n+1} - E_K^n}{\Delta t} + \sum_{\sigma\in\mathcal{E}_K} G_{K,\sigma}^{n+1} = -S_K^{n+1} + \sum_{\sigma\in\mathcal{E}_K} m(\sigma)R_{K,\sigma}^{n+1}, \quad (3.13)$$

where $m(\sigma)R_{K,\sigma}^{n+1} = \overline{F}_{K,\sigma}^{n+1} - \mathbf{F}_{K,\sigma}^{n+1} = O(h^2)$.

Multiplying (3.13) by E_K^{n+1}, and summing up the resulting products for $K \in \mathcal{J}$, we get

$$\begin{aligned} &\frac{1}{\Delta t}\sum_{K\in\mathcal{J}}(E_K^{n+1} - E_K^n)E_K^{n+1}m(K) + \sum_{K\in\mathcal{J}}\sum_{\sigma\in\mathcal{E}_K} G_{K,\sigma}^{n+1}E_K^{n+1} \\ &\quad = -\sum_{K\in\mathcal{J}} S_K^{n+1}E_K^{n+1} + \sum_{K\in\mathcal{J}}\sum_{\sigma\in\mathcal{E}_K} m(\sigma)R_{K,\sigma}^{n+1}E_K^{n+1}. \end{aligned}$$

Define the discrete L^2-norm and H^1-seminorm as follows:

$$\|E^n\|_2^2 = \sum_{K\in\mathcal{J}} |E_K^n|^2 m(K), \quad \|\nabla_\sigma E^n\|_2^2 = \sum_{\sigma\in\mathcal{E}} \tau_\sigma^n |\nabla_\sigma E^n|^2,$$

where $\nabla_\sigma E^n = |E_K^n - E_L^n|$, for $\sigma = K|L \in \mathcal{E}_{\text{int}}$; and $\nabla_\sigma E^n = |E_K^n|$, for $\sigma = K|L \in \mathcal{E}_K \cap \mathcal{E}_{\text{ext}}$. Denote $R_\sigma^n = |R_{K,\sigma}^n|$, and notice that for $\sigma = K|L \in \mathcal{E}_{\text{int}}$, we have $R_{K,\sigma}^n = -R_{L,\sigma}^n$. Hence, there is

$$\begin{aligned} &\frac{1}{2\Delta t}(\|E^{n+1}\|_2^2 - \|E^n\|_2^2) + \|\nabla_\sigma E^{n+1}\|_2^2 + \mathbf{E} \\ &\quad \leqslant \sum_{K\in\mathcal{J}} |S_K^{n+1}||E_K^{n+1}| + \sum_{\sigma\in\mathcal{E}} m(\sigma)R_\sigma^{n+1}\nabla_\sigma E^{n+1} \\ &\quad \leqslant \frac{1}{2}\|E^{n+1}\|_2^2 + \frac{1}{4}\|\nabla_\sigma E^{n+1}\|_2^2 + C(\Delta t + h)^2, \end{aligned} \quad (3.14)$$

where

$$\mathbf{E} = \sum_{\sigma\in\mathcal{E}_{\rm int}^o} \tau_\sigma^{n+1} D_\sigma (e_p^{n+1} - e_q^{n+1})(E_K^{n+1} - E_L^{n+1}) + \sum_{\sigma\in\mathcal{E}_{\rm int}, q\in\partial\Omega} \tau_\sigma^{n+1} D_\sigma e_p^{n+1} (E_K^{n+1} - E_L^{n+1}) - \sum_{\sigma\in\mathcal{E}_{\rm int}, p\in\partial\Omega} \tau_\sigma^{n+1} D_\sigma e_q^{n+1} (E_K^{n+1} - E_L^{n+1}).$$

Apply the assumption (V) to obtain

$$\mathbf{E} \leqslant \frac{1}{4}\|\nabla_\sigma E^{n+1}\|_2^2 + \sum_{\sigma\in\mathcal{E}} \tau_\sigma^{n+1} |D_\sigma|^2 (e_p^{n+1} - e_q^{n+1})^2 \leqslant \frac{1}{4}\|\nabla_\sigma E^{n+1}\|_2^2 + C\|\nabla_\gamma e^{n+1}\|_2^2. \quad (3.15)$$

Combine (3.14) and (3.15) to obtain

$$\|E^{n+1}\|_2^2 + \|\nabla_\sigma E^{n+1}\|_2^2 \Delta t \leqslant \frac{1}{1-\Delta t}\|E^n\|_2^2 + \frac{C\Delta t}{1-\Delta t}\|\nabla_\gamma e^{n+1}\|_2^2 + \frac{C\Delta t}{1-\Delta t}(\Delta t + h)^2.$$

Using discrete Gronwall inequality and Lemma 3, we obtain

$$\begin{aligned}\|E^{n+1}\|_2^2 + \sum_{k=0}^{n} \|\nabla_\sigma E^{k+1}\|_2^2 \Delta t &\leqslant C\bigg(\|E^0\|_2^2 + \sum_{k=0}^{n} \|\nabla_\gamma e^{k+1}\|_2^2 \Delta t + (\Delta t + h)^2\bigg) \\ &\leqslant C(\Delta t + h)^2. \end{aligned} \quad (3.16)$$

Thus, we have proved the following convergence theorem:

Theorem 1. *Assume* (I)–(V) *are satisfied. Then for the nine point scheme* (2.4), *there exists a constant C, independent of h, such that*

$$\|E^{n+1}\|_2^2 + \sum_{k=0}^{n} \|\nabla_\sigma E^{k+1}\|_2^2 \Delta t \leqslant C(\Delta t + h)^2, \quad 0 \leqslant n \leqslant N.$$

4 Numerical experiments

In this section we present the numerical results obtained on different meshes for several test problems. Four different types of meshes are used. One is a uniform mesh for the domain $\Omega = [0,1]\times[0,1]$. The number of cell center unknowns in the x and y directions are I and J, respectively, and therefore the total number of mesh points is $(I+1)\times(J+1)$. The other three meshes are distorted meshes. The first distorted mesh is a mesh with a sine domain (see Figure 5) defined as $\Omega = \{(x,y)|0 \leqslant x \leqslant 1, 0 \leqslant y \leqslant Y(x)\}$, where $Y(x) = 1 + \sin(2\pi x)/2$. The mesh is defined as

$$x_{ij} = \frac{i}{I}, \quad y_{ij} = \frac{jY(x_{ij})}{J},$$

$$i = 0, 1, \ldots, I, \quad j = 0, 1, \ldots, J.$$

The second distorted mesh is a Z-mesh (see Figure 6). The third distorted mesh is a random mesh. The random mesh over the physical domain $\Omega = [0,1]\times[0,1]$ is defined by

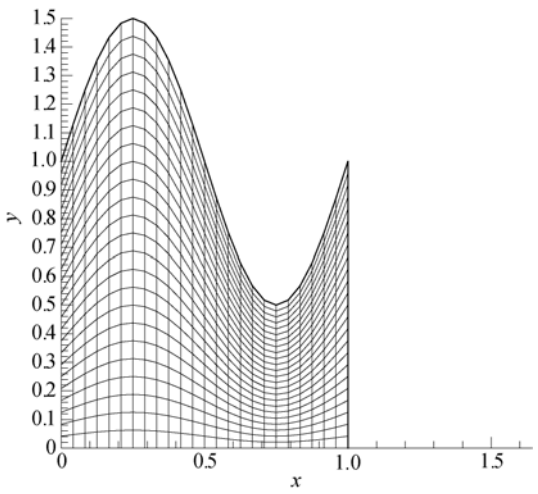

Figure 5 Sin-mesh

$$x_{ij} = \frac{i}{I} + \frac{\sigma}{I}(R_x - 0.5), \qquad y_{ij} = \frac{i}{J} + \frac{\sigma}{J}(R_y - 0.5),$$

where $\sigma \in [0, 1]$ is a parameter and R_x and R_y are two normalized random variables. When $\sigma = 0$ the mesh is uniform, and when σ is close to one it can become highly skewed. Figure 7 is a random mesh generated with $\sigma = 0.7$.

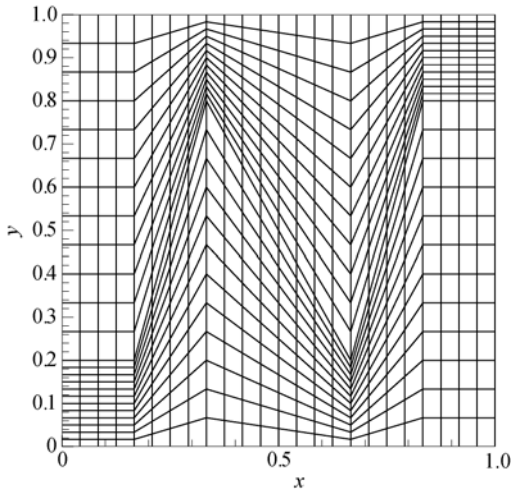

Figure 6 Z-mesh

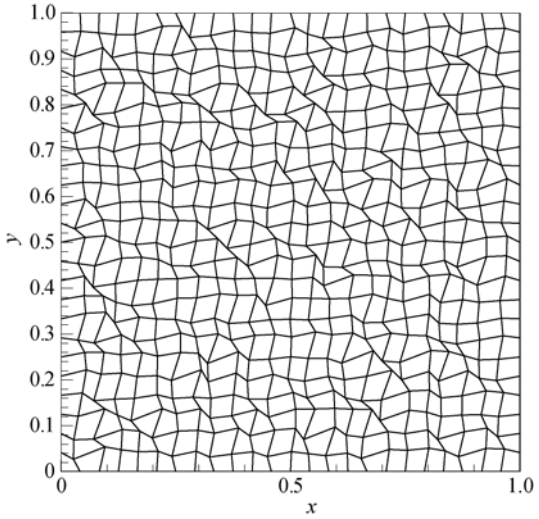

Figure 7 Random mesh

4.1 Linear elliptic equation

Consider the following linear elliptic equation

$$-\nabla \cdot (\nabla u) = \pi^2(\cos(\pi x) + \sin(\pi y)), \quad \text{in} \quad \Omega,$$
$$u = 2 + \cos(\pi x) + \sin(\pi y), \quad \text{on} \quad \partial\Omega.$$

The exact solution is $u = 2 + \cos(\pi x) + \sin(\pi y)$. In order to illustrate the accuracy of the method, we give in Table 1 the maximum error between the exact solution and the computed solution for the four meshes: uniform mesh, sin-mesh, Z-mesh and random mesh. From this table, we can see that the convergent rate is always larger than first order, and is near to second order for some cases.

Table 2 gives the numerical results obtained by the method in [10]. Compared Tables 1 and 2, we can see that the method of this paper provides more accurate results than the method in [10].

Table 1 Results for the linear elliptic equation

	$I \times J$	6×6	12×12	24×24	48×48	96×96
Uniform mesh	Maximum error	3.54E−2	8.82E−3	2.20E−3	5.51E−4	1.38E−4
	Rate	–	2.00	2.00	2.00	2.00
Sin-mesh	Maximum error	6.47e−2	2.45e−2	8.02e−3	2.30e−3	6.16e−4
	Rate	–	1.40	1.61	1.80	1.90
Z-mesh	Maximum error	1.40e−1	4.04e−2	1.05e−2	2.70e−3	6.84e−4
	Rate	–	1.79	1.94	1.96	1.98
Random mesh	Maximum error	4.72e−2	1.30e−2	4.37e−3	1.11e−3	3.08e−4
	Rate	–	1.86	1.57	1.98	1.85

Table 2 Results of the method in [10] for the linear elliptic equation

	$I \times J$	6×6	12×12	24×24	48×48	96×96
Uniform mesh	Maximum error	3.54E−2	8.82E−3	2.20E−3	5.51E−4	1.38E−4
	Rate	–	2.00	2.00	2.00	2.00
Sin-mesh	Maximum error	6.21e−2	2.59e−2	8.23e−3	2.34e−3	6.23e−4
	Rate	–	1.26	1.65	1.81	1.91
Z-mesh	Maximum error	1.69e−1	5.38e−2	1.46e−2	3.71e−3	9.23e−4
	Rate	–	1.65	1.88	1.98	2.01
Random mesh	Maximum error	6.74e−2	1.43e−2	3.78e−3	1.19e−3	3.18e−4
	Rate	–	2.24	1.92	1.67	1.90

4.2 Linear elliptic equation with discontinuous coefficient

Consider the following linear elliptic equation with discontinuous coefficient,

$$-\nabla \cdot (\kappa(x,y) \cdot \nabla u) = f(x,y), \qquad \text{in} \quad \Omega,$$

where

$$\kappa(x,y) = \begin{cases} 4, & (x,y) \in \left(0, \dfrac{2}{3}\right] \times (0,1), \\ 1, & (x,y) \in \left(\dfrac{2}{3}, 1\right) \times (0,1), \end{cases}$$

and

$$f(x,y) = \begin{cases} 20\pi^2 \sin \pi x \sin 2\pi y, & (x,y,t) \in \left(0, \dfrac{2}{3}\right] \times (0,1), \\ 20\pi^2 \sin 4\pi x \sin 2\pi y, & (x,y,t) \in \left(\dfrac{2}{3}, 1\right) \times (0,1). \end{cases}$$

The exact solution of the problem is

$$u(x,y,t) = \begin{cases} \sin \pi x \sin 2\pi y, & (x,y,t) \in \left(0, \dfrac{2}{3}\right] \times (0,1), \\ \sin 4\pi x \sin 2\pi y, & (x,y,t) \in \left(\dfrac{2}{3}, 1\right) \times (0,1), \end{cases},$$

and the Dirichlet boundary condition is used.

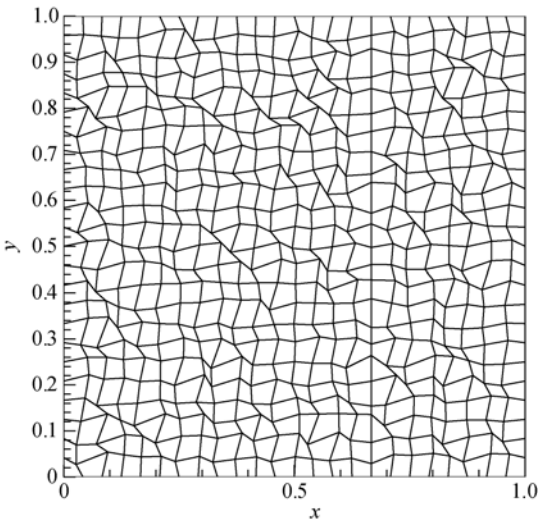

Figure 8 Random mesh with a discontinuity in $x = 2/3$

Since κ is discontinuous across $x = 2/3$, we use the randomly distorted mesh shown in Figure 8. Hence each primary element is homogeneous, but material properties vary across $x = 2/3$. In Table 3, we show the maximum error between the exact solution and the numerical solution for the four meshes: uniform mesh, sin-mesh, Z-mesh and random mesh with a discontinuity. From this table, we can see that the convergent rate of our scheme is higher than first order on the four meshes.

Then we present the numerical results obtained by the method in [11]. Compared Tables 3 and 4, we can see that the method of

Table 3 Results for the linear elliptic equation with discontinuous coefficient

	$I \times J$	6×6	12×12	24×24	48×48	96×96
Uniform mesh	Maximum error	2.90e−1	7.36e−2	2.36e−2	6.50e−3	1.69e−3
	Rate	–	1.98	1.64	1.86	1.94
Sin-mesh	Maximum error	2.67e−1	1.52e−1	4.91e−2	1.31e−2	4.10e−3
	Rate	–	0.82	1.63	1.91	1.68
Z-mesh	Maximum error	4.76e−1	1.29e−1	5.55e−2	1.90e−2	5.72e−3
	Rate	–	1.88	1.21	1.55	1.73
Random mesh	Maximum error	7.05e−1	1.40e−1	4.53e−2	1.16e−2	2.89e−3
	Rate	–	2.33	1.63	1.97	2.00

Table 4 Results of the method in [11] for the linear elliptic equation with discontinuous coefficient

	$I \times J$	6×6	12×12	24×24	48×48	96×96
Uniform mesh	Maximum error	3.11e−1	7.66e−2	2.36e−2	6.50e−3	1.69e−3
	Rate	–	2.02	1.70	1.86	1.94
Sin-mesh	Maximum error	6.08e−1	1.93e−1	5.93e−2	1.61e−2	4.99e−3
	Rate	–	1.66	1.70	1.88	1.69
Z-mesh	Maximum error	9.73e−1	6.44e−1	1.36e−1	3.93e−2	1.81e−2
	Rate	–	0.60	2.24	1.79	1.12
Random mesh	Maximum error	7.45e−1	1.81e−1	3.53e−2	1.12e−2	3.13e−3
	Rate	–	2.04	2.36	1.66	1.84

this paper also provides more accurate results than the method in [11] for this test problem.

4.3 Linear parabolic equation

Consider the following linear parabolic equation whose exact solution is $u = e^{-\pi^2 t}(2+\cos(\pi x)+\sin(\pi y))$:

$$u_t - \nabla \cdot (\nabla u) = -2\pi^2 e^{-\pi^2 t}, \quad \text{in} \quad \Omega,$$
$$u = e^{-\pi^2 t}(2 + \cos(\pi x) + \sin(\pi y)), \quad \text{on} \quad \partial\Omega.$$

In this computation, the time step size is chosen as $\Delta t = 1.0\mathrm{E} - 5$. With this small time step size, the time discretization error in our results can be ignored compared to the error from spatial discretization. We also give the error on four different meshes in Table 5. From this table, we can see that the method also recovers second-order convergence.

Table 5 Results for the linear parabolic equation ($T = 0.1$)

	$I \times J$	6×6	12×12	24×24	48×48	96×96
Uniform mesh	Maximum error	1.32e−1	3.71e−2	9.56e−3	2.41e−3	6.04e−4
	Rate	–	1.83	1.96	1.99	2.00
Sin-mesh	Maximum error	1.06e−1	3.00e−2	7.97e−3	2.21e−3	5.97e−4
	Rate	–	1.82	1.91	1.85	1.89
Z-mesh	Maximum error	1.89e−1	5.30e−2	1.34e−2	3.36e−3	8.40e−4
	Rate	–	1.84	1.99	2.00	2.00
Random mesh	Maximum error	1.35e−1	3.90e−2	9.89e−3	2.59e−3	6.66e−4
	Rate	–	1.79	1.98	1.93	1.96

5 Conclusion

By introducing the new method of calculating the vertex unknowns of nine point scheme on quadrilateral meshes for diffusion equations, the accuracy of the nine point scheme is improved. The advantage of this method is that it is particularly suitable for solving diffusion problems with discontinuous coefficients on highly distorted meshes, and it leads to a symmetric positive definite matrix. The method is proved to be first-order convergent on distorted meshes. Numerical experiments show that the method obtains nearly second-order accuracy on distorted meshes.

References

1 Eymard R, Gallouët T, Herbin R. Finite Volume Methods. In: Ciarlet P G, Lions J L, eds. Handbook of Numerical Analysis. Amsterdam: North Holland, 2000, 713–1020
2 Mishev I D. Finite volume methods on voronoï meshes, *Numer Methods PDEs*, **14**: 193–212 (1998)
3 Li D Y, Shui H S, Tang M J. On the finite difference scheme of two-dimensional Parabolic equation in a Non-Rectangular Mesh. *J Numer Methods Comput Appl*, **1**: 217–224 (1980)
4 Huang W Z, Kappen A M. A study of Cell-Center Finite Volume Methods for Diffusion Equations, Mathematics Research Report, 98-10-01, Lawrence University of Kansas, 1998
5 Li R H, Chen Z Y, Wu W. Generalized Difference Methods for Differential Equations, Numerical Analysis of Finite Volume Methods, Monographs and textbooks in pure and applied mathematics, 2000, 226
6 Wu J M, Fu S W, Shen L J. A difference scheme with high resolution for the numerical solution of nonlinear diffusion equation. *J Numer Methods Comput Appl*, **24**: 116–128 (2003)
7 Morel J E, Roberts R M, Shashkov M J. A local support-operators diffusion discretization scheme for quadrilateral r-z meshes. *J Comput Phys*, **144**: 17–51 (1998)
8 Lipnikov K, Morel J, Shashkov M. Mimetic finiteic finite difference methods for diffusion equations on non-orthogonal non-conformal Meshes. *J Comput Phys*, **199**: 589–597 (2004)
9 Aavatsmark I. An introduction to multipoint flux approximations for quadrilateral grids. *Comput Geosci*, **6**: 405–432 (2002)
10 Hermeline F. A finite volume method for the approximation of diffusion operators on distorted meshes. *J Comput Phys*, **160**: 481–499 (2000)
11 Yuan G W, Sheng Z Q. Analysis of accuracy of a finite volume scheme for diffusion equations on distorted meshes. *J Comput Phys*, **224**: 1170-1189 (2007)
12 Sheng Z Q, Yuan G W. A nine point scheme for the approximation of diffusion operators on distorted quadrilateral meshes. *SIAM J Sci Comput*, **30**: 1341–1361 (2008)
13 de Berg M, van Kreveld M, Overmars M, et al. Computational Geometry: Algorithms and Applications 2nd Edition. Berlin-Heidelberg-New York: Springer-Verlag, 2000